URSI GASS 2021, Rome, Italy, 28 August - 4 September 2021

Efficient low-cost system for monitoring the fiber-induced delay-shift within Radio Astronomic Scenarios

Jacopo Nanni*(1), Simone Rusticelli(2), Federico Perini(2), Jader Monari(2),
Enrico Lenzi(3), Mark Waterson(4) and Giovanni Tartarini(1)
(1) DEI-University of Bologna, Viale del Risorgimento 2, 40136 Bologna (BO), Italy
(2) Institute of Radio Astronomy, National Institute for Astrophysics, Via Fiorentina 3513, 40059 Medicina (BO), Italy
(3) Protech S.a.S, Via dei Pini 21, 31033 Castelfranco Veneto (TV), Italy
(4) SKA Organisation, Jodrell Bank, Macclesfield SK11 9FT, UK

Abstract

In the framework of radio astronomic systems, and in particular in the realization of the Aperture Array Verification Systems of the low frequency part of the Square Kilometre Array project, a monitoring of the delay introduced by the fiber optic cable of the antenna downlink is necessary in order to properly calibrate the receiver chain. A simple and relatively low-cost system is here proposed, which can directly provide such measurement without the use of complex post-processing systems, with precision estimated in 60ps for 6Km of fiber length.

1 Introduction

Due to its low attenuation, high bandwidth and immunity from electromagnetic interferences, the optical fiber is nowadays widely used for the downlink of Radio Telescopes antennas [1,2]. This is e.g. the case of the Square Kilometre Array (SKA), which is one of the major radio telescopes currently under development [3-5].
SKA will consist of two subsystems, one operating in the range 50-350 MHz, named SKA-LOW and the other operating from 350MHz to 14GHz, named SKA-MID. In the frame of SKA-LOW, which will be composed of more than 130.000 antennas, and of its current Aperture Array Verification System (AAVS), composed of a few hundred ones, Radio over Fiber (RoF) downlinks having a maximum length of 6Km are utilized. In this context, the verification and stable calibration of the fiber-induced delay, and of its possible shift induced by external agent variations (temperature *in primis*), is one of the major objectives to be pursued, with a required resolution lower than 100 psec.
This work proposes a simple and low-cost system capable to measure the above-mentioned delay shifts, so that it will be possible to adopt it within AAVS and SKA-LOW systems, and, more in general, in a variety of optical fiber-based sensing applications.

2 Principle of the system proposed

The system proposed is based on a *Michelson-like* interferometer and is illustrated in Figure 1. It is composed of a laser source coupled with a short pigtail of standard G.652 fiber connected to a balanced (50/50) coupler where the two outputs are connected to two different spans of fibers of length L_1 and L_2.

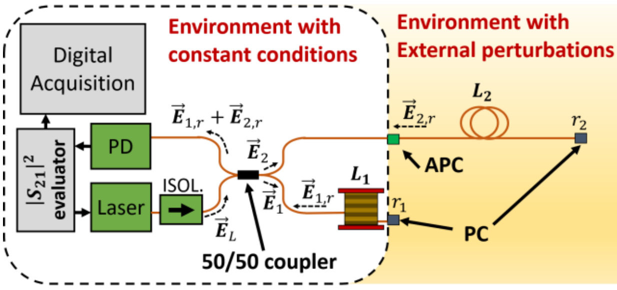

Figure 1 Interferometric system proposed**.** See text for details.

In particular, the fiber of length L_2 is considered as placed in an external environment, subject to several stresses such as temperature and mechanical ones, while the other fiber of length L_1 is placed in an environment with constant conditions. The two fibers are then terminated with straight Physical Contact (PC) connectors which provide a reflection of the electrical field. The two reflected fields $\vec{E}_{1,r}(t)$ and $\vec{E}_{2,r}(t)$ are then re-combined by the initial balanced coupler, being received by a photodetector at the upper branch being blocked by an opto-isolator at the lower one. The RF frequency response of such system is then evaluated by a scalar network analyzer, being able to evaluate the quantity $|S_{21}|^2$. As will be shown in detail hereafter, the response of such system is composed of several maxima and minima on the frequency domain, whose positions directly depend on the electromagnetic and geometric characteristics of the fiber, leading to a very precise measurement of fiber delay shifts induced by external perturbations.
To mathematically describe the system operation, a laser source is considered, which emits at the angular optical frequency ω_0 and is directly modulated by an RF sinusoidal current having amplitude I_{RF} and angular frequency ω_{RF}. The laser is equipped with a short pigtail of standard single-mode fiber where the expression of the electrical field can be written at the input section as:

$$\vec{E}_L(t) = E_0\sqrt{1 + m_i \cos(\omega_{RF} t)}\ e^{j[\omega_0 t + \theta(t) + \phi(t)]}\ \vec{e}_L \quad (1)$$

where E_0 is electrical field amplitude, $\vec{e}_L$is the polarization unit vector, m_i is the optical modulation index, $\theta(t)$ is the spurious phase modulation due to the direct modulation and $\phi(t)$ is the phase noise of the laser.
After passing through the balanced coupler, the field is equally split into two separate fields $\vec{E}_1$ and $\vec{E}_2$ travelling in the two branches of length L_1 and L_2, with attenuation coefficients α_1 and α_2 and group delays τ_1 and τ_2, respectively. The two fields are then reflected with field reflection coefficients r_1 and r_2 by the two PC connectors. Therefore, before passing through the balanced coupler the expressions of $\vec{E}_{1,r}(t)$ and $\vec{E}_{2,r}(t)$ read as:

$$\vec{E}_{1,r}(t) = r_1 \frac{E_0}{\sqrt{2}} \sqrt{1 + m_i \cos[\omega_{RF}(t - 2\tau_1)]} \cdot \cdot e^{-\alpha_1 L_1 + j[\omega_0(t-2\tau_1) + \theta(t-2\tau_1) + \phi(t-2\tau_1)]}\, \vec{e}_1 \quad (2)$$

$$\vec{E}_{2,r}(t) = r_2 \frac{E_0}{\sqrt{2}} \sqrt{1 + m_i \cos[\omega_{RF}(t - 2\tau_2)]} \cdot \cdot e^{-\alpha_2 L_2 + j[\omega_0(t-2\tau_2) + \theta(t-2\tau_2) + \phi(t-2\tau_2)]}\, \vec{e}_2 \quad (3)$$

After passing through the coupler the sum of the two fields arrives at the photodetector, having surface S_{PD} and responsivity R, generating the current:

$$\begin{aligned} i_{PD} &= R \int_{S_{PD}} \left| \frac{\vec{E}_{1,r} + \vec{E}_{2,r}}{\sqrt{2}} \right|^2 dS = \\ &= r_1^2 \frac{RP_0}{4} e^{-2\alpha_1 L_1} \{1 + m_i \cos[\omega_{RF}(t - 2\tau_1)]\} \\ &+ r_2^2 \frac{RP_0}{4} e^{-2\alpha_2 L_2} \{1 + m_i \cos[\omega_{RF}(t - 2\tau_2)]\} \\ &+ q r_1 r_2 \frac{P_0}{2} e^{-(\alpha_1 L_1 + \alpha_2 L_2)} \\ & R\sqrt{1 + m_i \cos[\omega_{RF}(t - 2\tau_1)]} \sqrt{1 + m_i \cos[\omega_{RF}(t - 2\tau_2)]} \\ &\cdot \cos[\omega_0(2\tau_2 - 2\tau_1) + \theta(t - 2\tau_1) - \theta(t - 2\tau_2) \\ &+ \phi(t - 2\tau_1) - \phi(t - 2\tau_2)] \end{aligned} \quad (4)$$

where $q = \int \vec{e}_1 \cdot \vec{e}_2^* \, dS$ represents the polarization matching factor.
Considering the last side of Eq.(4), the current i_{PD} is composed of the first two terms which are independent from the electric fields' phases and by the last term which depends on the difference of the phases of the two fields. This last term accounts in general for the interference of the two optical signals, and can be usefully exploited in some cases to evaluate some quantities of the optical link [6,7]. In the present case it however results to have a negligible impact in the determination of i_{PD}.
Indeed, if $2 \cdot (\tau_2 - \tau_1) > \tau_{coh}$, where τ_{coh} is the coherence time of the source, it is possible to demonstrate that such term produces at frequency ω_{RF} a small amount of power compared to the other two terms, due to the presence of the difference of uncorrelated phases $\phi(t - 2\tau_1) - \phi(t - 2\tau_2)$ with gaussian statistics within the cosine argument. Note that the condition above can be also expressed as $2|L_2 - L_1| = 2\Delta L \geq l_{coh}$, where $l_{coh} = v_{gn}\tau_{coh}$ represents the coherence length of the source, and where v_{gn} is the nominal value of the group velocity of the fundamental mode, given by the supplier. In such conditions the photo-current i_{PD} can be approximated as:

$$\begin{aligned} i_{PD} &\simeq R \int_{S_{PD}} \left| \frac{\vec{E}_{1,r} + \vec{E}_{2,r}}{\sqrt{2}} \right|^2 dS = \\ &= r_1^2 \frac{RP_0}{4} e^{-2\alpha_1 L_1} \{1 + m_i \cos[\omega_{RF}(t - 2\tau_1)]\} \\ &+ r_2^2 \frac{RP_0}{4} e^{-2\alpha_2 L_2} \{1 + m_i \cos[\omega_{RF}(t - 2\tau_2)]\} \end{aligned} \quad (5)$$

Considering now, for simplicity but without loss of generality, $r_1^2 = r_2^2 = r^2$ and $\alpha_1 L_1 \simeq \alpha_2 L_2 \simeq \alpha L$, the expression of i_{PD} simplifies as:

$$\begin{aligned} i_{PD} \simeq \frac{r^2 RP_0}{4} e^{-2\alpha L} \{2 &+ m_i \cos[\omega_{RF}(t - 2\tau_1)] \\ &+ m_i \cos[\omega_{RF}(t - 2\tau_2)]\} \end{aligned} \quad (6)$$

Then, applying a well-known trigonometric identity, it is possible to write the PD current as follows:

$$\begin{aligned} i_{PD} = i_{PD,DC} + i_{PD,\omega_{RF}} & \\ &= \frac{r^2 RP_0}{2} e^{-2\alpha L} \\ &+ m_i \frac{r^2 RP_0}{2} e^{-2\alpha L} \cos[\omega_{RF}(\tau_1 - \tau_2)] \\ &\cdot \cos[\omega_{RF}(t - (\tau_1 + \tau_2))] \end{aligned} \quad (7)$$

Finally, the measured frequency response $|S_{21}(\omega_{RF})|^2$ can be computed as:

$$\begin{aligned} |S_{21}(\omega_{RF})|^2 &= \frac{< i_{PD,\omega_{RF}}^2 >}{I_{RF}^2} = \\ &= \frac{R^2 r^4 \eta_{TX}^2(\omega_{RF})}{8} e^{-4\alpha L} |\cos[\omega_{RF} \Delta(\hat{\tau} L)]|^2 \end{aligned} \quad (8)$$

Where $\eta_{TX}^2(\omega_{RF})$ is the frequency modulation response of the laser at $\omega = \omega_{RF}$ and $\hat{\tau}_1, \hat{\tau}_2$ represent the group delays-per-unit-meter (i.e. the reciprocal of the group velocities) of the fundamental modes in reference fiber and fiber under test, respectively. For simplicity it has been also put $\Delta(\hat{\tau} L) = \hat{\tau}_2 L_2 - \hat{\tau}_1 L_1$.
According to Eq.(8), at the frequencies described by the law:

$$f_{RF,min,k} = \frac{2k + 1}{4 \cdot \Delta(\hat{\tau} L)} \qquad k = 0,1,2, \ldots \quad (9)$$

$|S_{21}|^2$ presents minimum (theoretically zero) values, whose position depends directly on $\Delta(\hat{\tau} L)$. This means that it is sufficient to track the position of one of these minima to obtain the behavior of the delay difference between the reference fiber and the fiber under test (see Figure 2).

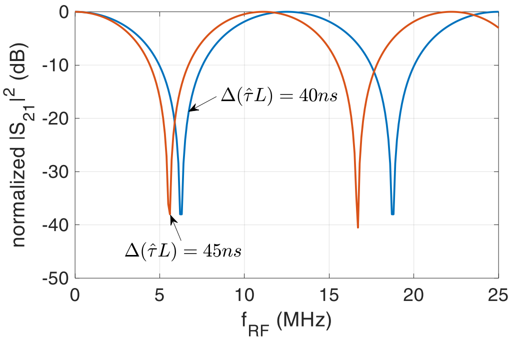

Figure 2 Typical normalized behavior of $|S_{21}(\omega_{RF})|^2$ for two different values of $\Delta(\hat{\tau}L)$.

Supposing that the fiber of length L_1 is located at temperature $T_1(t)$ and the one of length L_2 is located at temperature $T_2(t)$, the term $\Delta(\hat{\tau}L)$ can be expanded in the following form:

$$\Delta(\hat{\tau}L) = (\hat{\tau}_2 L_2)_{|T_2=T_{2,0}} + \delta(\hat{\tau}_2 L_2) - \left[(\hat{\tau}_1 L_1)_{|T_1=T_{1,0}} + \delta(\hat{\tau}_1 L_1)\right] \qquad (10)$$

where $T_{2,0} = T_2(t_0)$, $T_{1,0} = T_1(t_0)$ represent the initial temperatures in the two environments at the instant t_0, while $\delta(\hat{\tau}_2 L_2), \delta(\hat{\tau}_1 L_1)$ represent the perturbation introduced by possible temperature variations δT_1, δT_2, respectively.

If we suppose that the environmental conditions in which the fiber of length L_1 is placed are stable (i.e., $\delta T_1 \simeq 0$), it is possible to assume $\delta(\hat{\tau}_1 L_1) \simeq 0$, so that the expression of $\Delta(\hat{\tau}L)$ simplifies as follows:

$$\Delta(\hat{\tau}L) = \left[(\hat{\tau}_2 L_2)_{|T_2=T_{2,0}} - (\hat{\tau}_1 L_1)_{|T_1=T_{1,0}}\right] + \delta(\hat{\tau}_2 L_2) = \Delta(\hat{\tau}L)_{\substack{|T_1=T_{1,0} \\ |T_2=T_{2,0}}} + \delta(\hat{\tau}_2 L_2) \qquad (11)$$

meaning that if the fiber of length L_1 is subject to adequately smaller temperature variations compared to fiber of length L_2, the changes in the frequencies of the minima, and therefore in $\Delta(\hat{\tau}L)$, depend exclusively by the changes occurred in the fiber exposed to environmental perturbations.

3 Experimental Test of the system

To validate the system proposed the setup of Figure 3 has been used. A 10mW 1550nm Distributed Feed-Back (DFB) laser equipped with Thermo-Electric Cooler (TEC) and opto-isolator has been utilized as electro-optical source, while as opto-electrical receiver a PIN-PD followed by an LNA with 42dB Gain has been employed. Then, to replicate the order of distances involved in AAVS, two fibers of 6Km nominal length have been employed, where the one with length L_2 has been placed within a climatic chamber. The two fiber lengths have then been tested using a commercial Optical Time Domain Reflectometry (OTDR) from VIAVI where it has been found that $L_1 = 6095m$, $L_2 = 6240m$ leading to $\Delta L = 145m$ at $T_1 = T_2 \simeq 20$ °C.

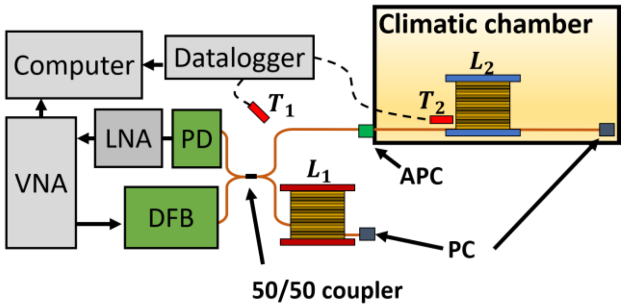

Figure 3 Experimental setup employed. See text for details.

Note that considering a typical value of DFB coherence length $l_{coh} \simeq 15m$ the condition $2\Delta L > l_{coh}$ is widely respected. The temperatures are monitored using two different Resistance Temperature Detectors (RTDs) connected to a datalogger controlled via computer. Finally, to measure $|S_{21}(\omega_{RF})|^2$, a Vectorial Network Analyzer (VNA) has been utilized.
As a first step, it is necessary to choose the order of the minimum of $|S_{21}|^2$ to monitor and the range of frequencies around which to record its variations.
Regarding the first point, it is sufficient to estimate reference values of the various $f_{RF,min,k}$ from the length difference ΔL, considering in this case $\hat{\tau}_1 \simeq \hat{\tau}_2 \simeq \frac{1}{v_{gn}} = 4.92\frac{ns}{m}$, which leads to $\Delta(\hat{\tau}L) \simeq \Delta L / v_{gn} = 713ns$ and to $f_{RF,min,k|T_1=T_2=20°C} \simeq 350\,(2k+1)\,KHz$. One of these frequency values, corresponding to a minimum of a certain order k, must then be chosen to be tracked in time.
Instead, as frequency span of the measurement system $\Delta f_{RF,min|T_1=T_2=20°C}$ (a quantity which does not dependent on the order of the chosen minimum order k), the value was $\Delta f_{RF,min|T_1=T_2=20°C} \simeq 700\,KHz$ has been chosen.
With these two data, the VNA must be calibrated for working with a maximum span of $\Delta f_{RF,min|T_1=T_2=20°C}$, centered in one of the minima, depending on the frequency characteristics of the components adopted in the setup. In the present case $k=29$ has been chosen leading to a center frequency of $f_{RF,min,k|T_1=T_2=20°C} \simeq 19.6\,MHz$ where 801 points have been set to be measured by the VNA. After this first setting the climatic chamber has set for imposing a temperature ramp from -10°C to 50 °C in 500 minutes and turned on.
Figure 4 shows and example of frequency response obtained at different values of T_2. The full measurement of $\delta(\hat{\tau}_2 L_2)$ with respect T_2 is shown in Figure 5, where the behavior of T_2 versus time is also represented as inset, showing the forced temperature slope of about 0.12°C/min. The behavior of T_1 is also shown, presenting a mean value of 20.2°C, a standard deviation of 0.1 °C and a peak excursion of 0.6°C. The slope of the curve, normalized to the nominal length L_2, is about $39\frac{ps}{Km\,°C}$

which is quite in agreement with the theoretical expected value of 40 $\frac{ps}{Km\,°C}$ [8].

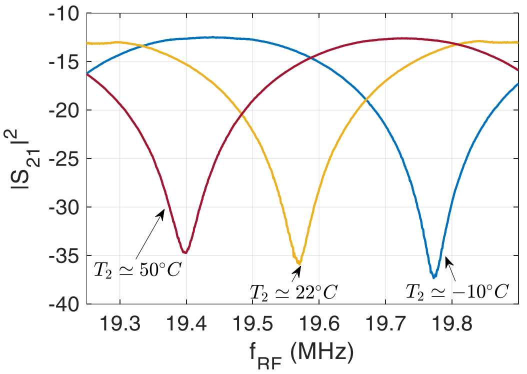

Figure 4 Example of frequency response obtained at different values of T_2.

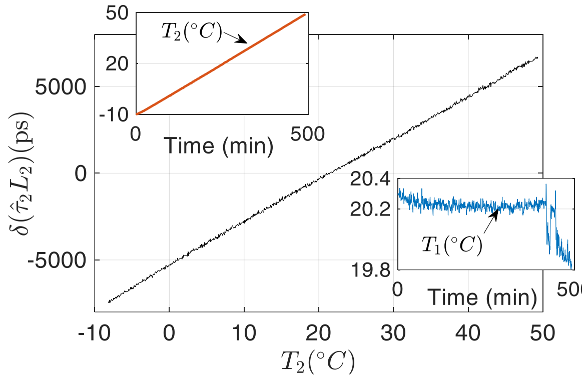

Figure 5 Measurement of $\delta(\hat{\tau}_2 L_2)$ forcing a temperature ramp in the climatic chamber from -10°C to 50°C within 500 min of duration (see inset). T_1 is also reported as inset.

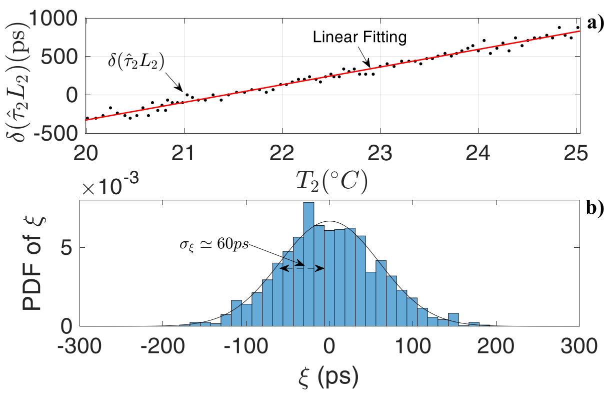

Figure 6 (a) Zoom of the measurement from 20°C to 25°C, showing the linear fitting used to estimate the precision of the method. (b) PDF of the error variable ξ.

Finally, Figure 6a shows a zoom of the results obtained between 20°C and 25°C showing the linear fitting applied which allows to estimate the precision of the method, computed as the deviation of the measurement points from such fitting. Defining the variable ξ as the difference between the measured values and the linear fitting ones, the Probability Density Function (PDF) of ξ results to be gaussian with zero-mean and standard deviation $\sigma_\xi \simeq 60ps$ (see Fig. 6b).

4 Conclusion

The proof-of-concept of a simple system, capable to monitor the temperature-induced delay-shift on fiber connections of some km length has been shown. The values obtained of delay variations agree with the theoretically expected values and show a standard deviation of about 60ps for a 6km link length. Considering that a reference fiber can be easily located in each substation, and that its length doesn't need to be critically matched to the length of the monitored fiber, this technique could be used in the SKA1-LOW to track delay and phase changes. Possibilities of improving the system performance, which will be part of future works, consist in increasing the resolution (at the price of a slowdown) of the measurement of $|S_{21}(\omega_{RF})|^2$ and/or using optical reflectors instead of PC connectors and/or employing a small amount of post-processing for taking into account the variation of the reference fiber.

5 References

1. P. Garcia-Carreño et al., "Geodetic VLBI ultra low noise broad-band receiver for 13 meter VGOS radiotelescopes," *46th European Microwave Conference (EuMC)*, London, 2016, pp. 1405-1408.

2. J. Nanni *et al.*, "Controlling Rayleigh-Backscattering-Induced Distortion in Radio Over Fiber Systems for Radioastronomic Applications," in *J. Lightw. Technol.*, vol. 38, no. 19, pp. 5393-5405, 1 Oct.1, 2020.

3. A. J. Faulkner and J. G. B. de Vaate, "SKA low frequency aperture array," in Proc. *IEEE Int. Symp. Antennas Propag. USNC/URSI Nat. Radio Sci. Meeting*, Jul. 2015, pp. 1368–1369

4. J. Nanni et al., "Challenges due to Rayleigh backscattering in radio over fibre links for the square kilometre array radio-telescope," in *Proc. 21st Int. Conf. Transparent Opt. Netw.,* Jul. 2019, pp. 1–4

5. J. Nanni et al., "Optimum mitigation of distortion induced by Rayleigh backscattering in radio-over-fiber links for the square kilometer array radio-telescope,"*Proc. Int. Topical Meeting Microw. Phot.*, Oct. 2019, pp. 1–4

6. J. Nanni *et al.*, "Chirp Evaluation of 850-nm Single Mode VCSEL Exploiting Modal Noise in Standard Single Mode Fiber," in *IEEE J. Quantum Electron.*, vol. 54, no. 4, pp. 1-11, Aug. 2018, Art no. 2400611.

7. J. Nanni *et al.*, "Chirp evaluation of semiconductor DFB lasers through a simple Interferometry-Based (IB) technique," *Appl. Opt.* 55, 7788-7795 (2016).

8. M. Bousonville and J. Rausch," Velocity of Signal Delay Changes in Fibre Cables," Proc. of DIPAC09, Basel, Switzerland, 2009.